Chapter 2
From Fourier Transform to Wavelet Transform: A Historical Perspective

To ensure safe and economical operation and product quality, manufacturing machines and processes are constantly monitored and evaluated for their working conditions, on the basis of signals collected by sensors, which are generally presented in the form of time series (e.g., time-dependent variation of vibration, pressure, temperature, etc.). To extract information from such signals and reveal the underlying dynamics that corresponds to the signals, proper signal processing technique is needed. Typically, the process of signal processing transforms a time-domain signal into another domain, with the purpose of extracting the characteristic information embedded within the time series that is otherwise not readily observable in its original form. Mathematically, this can be achieved by representing the time-domain signal as a series of coefficients, based on a comparison between the signal $x(t)$ and a set of known, template functions $\{\psi_n(t)\}_{n\in z}$ as (Chui 1992; Qian 2002)

$$c_n = \int_{-\infty}^{\infty} x(t)\psi_n^*(t)dt \tag{2.1}$$

where $(\cdot)^*$ stands for the complex conjugate of the function $(\cdot)$. The inner product between the two functions $x(t)$ and $\psi_n(t)$ is defined as

$$\langle x, \psi_n \rangle = \int x(t)\psi_n^*(t)dt \tag{2.2}$$

Then (2.1) can be expressed in the general form as

$$c_n = \langle x, \psi_n \rangle \tag{2.3}$$

The inner product in (2.3), in essence, describes an operation of comparing the "similarity" between the signal $x(t)$ and the template function $\{\psi_n(t)\}_{n\in z}$, that is, the degree of closeness between the two functions. The more similar $x(t)$ is to $\psi_n(t)$, the larger the inner product c_n will be. On the basis of this notion, this chapter presents a historical perspective on the evolution of the wavelet transform. This is realized by observing the similarities as well as differences between the wavelet

R.X. Gao and R. Yan, *Wavelets: Theory and Applications for Manufacturing*,
DOI 10.1007/978-1-4419-1545-0_2, © Springer Science+Business Media, LLC 2011

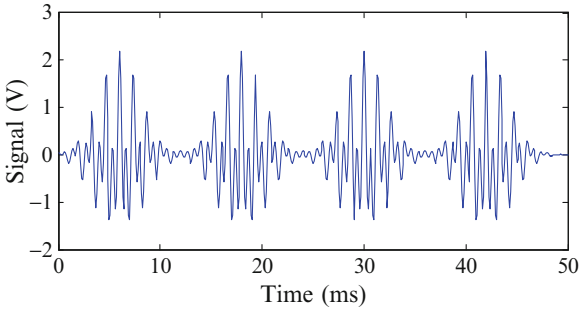

Fig. 2.1 A nonstationary signal $x(t)$

transform and other commonly used techniques, in terms of the choice of the template functions $\{\psi_n(t)\}_{n\in z}$. To illustrate the point, a nonstationary signal as shown in Fig. 2.1 is used as an example. The signal consists of four groups of impulsive signal trains, each containing two transient elements of different center frequencies at 1,500 and 650 Hz, respectively. The four groups are separated from one another by a 12-ms time interval. Within each group, the two transient elements are time-overlapped. The sampling frequency used to capture the signal is 10 kHz.

2.1 Fourier Transform

The Fourier transform is probably the most widely applied signal processing tool in science and engineering. It reveals the frequency composition of a time series $x(t)$ by transforming it from the time domain into the frequency domain. In 1807, the French mathematician Joseph Fourier (Fig. 2.2) found that any periodic signal can be presented by a weighted sum of a series of sine and cosine functions. However, because of the uncompromising objections from some of his contemporaries such as J. L. Lagrange (Herivel 1975), his paper on this finding never got published, until some 15 years later, when Fourier wrote his own book, *The Analytical Theory of Heat* (Fourier 1822). In that book, Fourier extended his finding to aperiodic signals, stating that an aperiodic signal can be represented by a weighted integral of a series of sine and cosine functions. Such an integral is termed the Fourier transform.

Using the notation of inner product, the Fourier transform of a signal $x(t)$ can be expressed as

$$X(f) = \langle x, e^{i2\pi ft} \rangle = \int_{-\infty}^{\infty} x(t) e^{-i2\pi ft}\, dt \tag{2.4}$$

"An arbitrary function, continuous or with discontinuities, defined in a finite interval by an arbitrarily capricious graph can always be expressed as a sum of sinusoids"
J.B.J. Fourier

Fig. 2.2 Jean B. Joseph Fourier (1768–1830)

Assuming that the signal has finite energy,

$$\int_{-\infty}^{\infty} |x(t)|^2 dt < \infty$$

Accordingly, the inverse Fourier transform of the signal $x(t)$ can be expressed as

$$x(t) = \int_{-\infty}^{\infty} X(f) e^{i2\pi ft} \, df \tag{2.5}$$

Signals obtained experimentally through a data acquisition system are generally sampled at discrete time intervals ΔT, instead of continuously, within a total measurement time T. Such a signal, defined as x_k, can be transformed into the frequency domain by using the discrete Fourier transform (DFT), defined as

$$DFT(f_n) = \frac{1}{N} \sum_{k=0}^{N-1} x_k e^{-i2\pi f_n k \Delta T} \tag{2.6}$$

where $N = T/\Delta T$ is the number of samples, and $f_n = n/T, n = 0, 1, 2, \ldots, N-1$ are the discrete frequency components. The inverse DFT can then be expressed as

$$x_k = \frac{1}{\Delta T} \sum_{f_n=0}^{(N-1)/T} DFT(f_n) e^{i2\pi f_n k \Delta T} \tag{2.7}$$

Equations (2.4) and (2.6) indicate that the Fourier transform is essentially a convolution between the time series $x(t)$ or x_k and a series of sine and cosine functions that can be viewed as template functions. The operation measures the similarity between $x(t)$ or x_k and the template functions, and expresses the average frequency information during the entire period of the signal analyzed. In Fig. 2.3, such an operation is graphically illustrated.

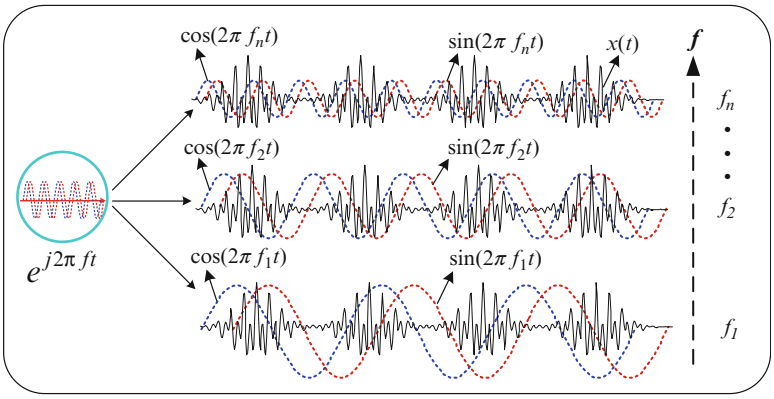

Fig. 2.3 Illustration of the Fourier transform of a continuous signal $x(t)$

To compute the DFT of a signal with N samples, multiplication of an $N \times N$ matrix that contains the primitive nth root of unity $e^{-i2\pi/N}$ by the signal is needed. Such an operation takes a total of arithmetic operations on the order of N^2 to complete. The computational time increases quickly as the number of the samples increases. For example, a time series of $N = 256$ (i.e., 2^8) samples takes 65,536 operational steps to complete, whereas for $N = 4{,}096$ (i.e., 2^{12}), a total of 16,777,216 steps will be needed to compute its DFT. The high computational cost limited the widespread application of the DFT in its early stage, until a more efficient algorithm, called the Cooley–Tukey algorithm, was introduced in 1965 (Cooley and Tukey 1965). This algorithm is also called the fast Fourier transform (FFT), and what it does is to recursively break down a DFT of a large data sample (i.e., a large N) into a series of smaller DFTs of smaller samples by dividing the transform with size N into two pieces of size $N/2$ at each step, and reduce the arithmetic operations to a total of $N \log(N)$. Comparing to the N^2 operations required for DFT, this represents a time reduction of up to 96%, when, for example, the data sample number N is 256.

In practice, the phenomena of *leakage* and *aliasing* can happen during the calculation of DFT (Körner 1988). Leakage is caused by the discontinuities involved when a signal is extended periodically for performing the DFT. Applying a window to the signal to force it to contain a full period can prevent leakage from happening. However, the window itself may contribute frequency information to the signal. Aliasing occurs when the Shannon's sampling theorem is violated, (Bracewell 1999) causing the actual frequency component to appear at different locations in the frequency spectrum. This can be solved by ensuring the sampling frequency to be at least twice as large as the maximum frequency component contained in the signal (Bracewell 1999). This requires, however, that the maximum frequency component is known a priori.

The Fourier transform of the signal shown in Fig. 2.1 is illustrated in Fig. 2.4. The figure shows two major frequency peaks at 650 and 1,500 Hz, respectively.

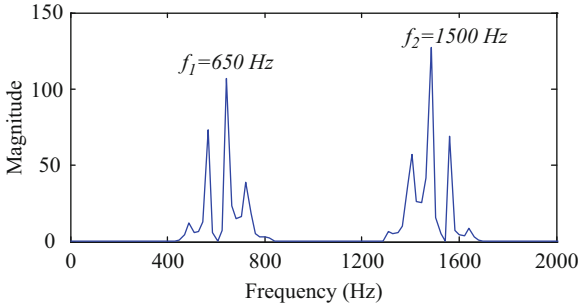

Fig. 2.4 Fourier transform results of the signal $x(t)$

However, it does not reveal how the signal's frequency contents vary with time; that is, the figure does not reveal if the two frequency components are continuously present throughout the time of observation or only at certain intervals, as is implicitly shown in the time-domain representation. Because the temporal structure of the signal is not revealed, the merit of the Fourier transform is limited; specifically, it is not suited for analyzing nonstationary signals. On the other hand, as signals encountered in manufacturing are generally nonstationary in nature (e.g., subtle, time-localized changes caused by structural defects are typically seen in vibration signals measured from rotary machines), a new signal processing technique that is able to handle the nonstationarity of a signal is needed.

2.2 Short-Time Fourier Transform

A straightforward solution to overcoming the limitations of the Fourier transform is to introduce an analysis window of certain length that glides through the signal along the time axis to perform a "time-localized" Fourier transform. Such a concept led to the short-time Fourier transform (STFT), introduced by Dennis Gabor (Fig. 2.5) in his paper titled "Theory of communication," published in 1946 (Gabor 1946).

As shown in Fig. 2.6, the STFT employs a sliding window function $g(t)$ that is centered at time τ. For each specific τ, a time-localized Fourier transform is performed on the signal $x(t)$ within the window. Subsequently, the window is moved by τ along the time line, and another Fourier transform is performed. Through such consecutive operations, Fourier transform of the entire signal can be performed. The signal segment within the window function is assumed to be approximately stationary. As a result, the STFT decomposes a time domain signal into a 2D time-frequency representation, and variations of the frequency content of that signal within the window function are revealed, as illustrated in Fig. 2.6.

Fig. 2.5 Dennis Gabor (1900–1979)

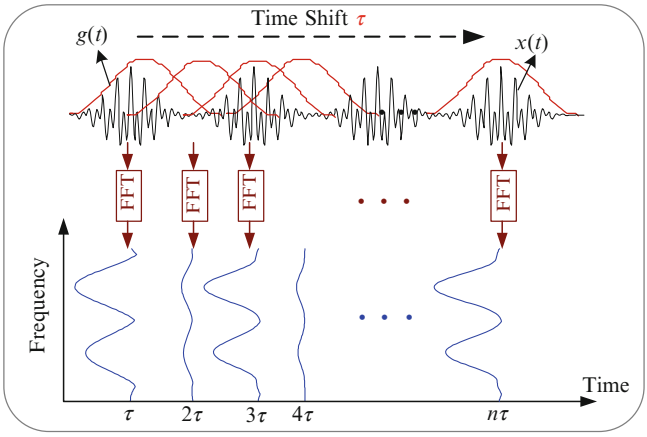

Fig. 2.6 Illustration of short-time Fourier transform on the test signal $x(t)$

Using the inner product notation as before, the STFT can be expressed as

$$STFT(\tau,f) = \langle x, g_{\tau,f} \rangle = \int x(t) g^*_{\tau,f}(t) dt = \int x(t) g(t-\tau) e^{-j2\pi ft}\, dt \qquad (2.8)$$

Equation (2.8) can also be viewed as a measure of "similarity" between the signal $x(t)$ and the time-shifted and frequency-modulated window function $g(t)$. Over the past few decades, various types of window functions have been developed (Oppenheim et al. 1999), and each of them is specifically tailored toward a particular type of application. For example, the Gaussian window designed for analyzing transient signals, and the Hamming and Hann windows are applicable to narrowband, random signals, and the Kaiser-Bessel window is better suited for separating two signal components with frequencies very close to each other but with widely differing amplitudes. It should be noted that the choice of the window function

directly affects the time and frequency resolutions of the analysis result. While higher resolution in general provides better separation of the constituent components within a signal, the time and frequency resolutions of the STFT technique cannot be chosen arbitrarily at the same time, according to the uncertainty principle (Cohen 1989). Specifically, the product of the time and frequency resolutions is lower bounded by

$$\Delta\tau \cdot \Delta f \geq \frac{1}{4\pi} \tag{2.9}$$

where $\Delta\tau$ and Δf denote the time and frequency resolutions, respectively. Analytically, the time resolution $\Delta\tau$ is measured by the root-mean-square time width of the window function, defined as

$$\Delta\tau^2 = \frac{\int \tau^2 |g(\tau)|^2 d\tau}{\int |g(\tau)|^2 d\tau} \tag{2.10}$$

Similarly, the frequency resolution Δf is measured by the root-mean-square bandwidth of the window function, and is defined as (Rioul and Vetterli 1991)

$$\Delta f^2 = \frac{\int f^2 |G(f)|^2 \, df}{\int |G(f)|^2 \, df} \tag{2.11}$$

In (2.11), $G(f)$ is the Fourier transform of the window function $g(t)$. As an example, the Gaussian window function $g(t) = \mathrm{e}^{-\alpha t^2 \tau^2}$ (with α being a constant and τ controlling the window width) has the time and frequency resolutions of $\Delta\tau = \tau/(2\sqrt{\alpha})$ and $\Delta f = \sqrt{\alpha}/(\tau \cdot 2\pi)$, respectively. As a result, the time-frequency resolution provided by the Gaussian window when analyzing a signal $x(t)$ is $\Delta\tau \cdot \Delta f = 1/4\pi$. As the time and frequency resolutions of a window function are dependent on the parameter τ only, once the window function is chosen, the time and frequency resolutions over the entire time-frequency plane are fixed. Illustrated in Fig. 2.7 are two scenarios where the products of the time and frequency resolutions of the window function (i.e., the area defined by the product of $\Delta\tau \cdot \Delta f$) are the same, regardless of the actual window size (τ or $\tau/2$) employed.

The effect of the window size τ on the time and frequency resolutions is illustrated in Fig. 2.8, where STFT with the Gaussian window was performed on the signal shown in Fig. 2.1. Altogether three different window sizes (i.e., 1.6, 6.4, and 25.6 ms) were chosen. While the smallest window width of 1.6 ms has provided high time resolution in separating the four pulse trains contained in the signal, as illustrated in Fig. 2.8a, its frequency resolution was too low to differentiate the two time-overlapped transient elements within each group. As a result, the frequency elements 1,500 and 650 Hz are displayed as one lumped group on the time-frequency plane. In contrast, the largest window width

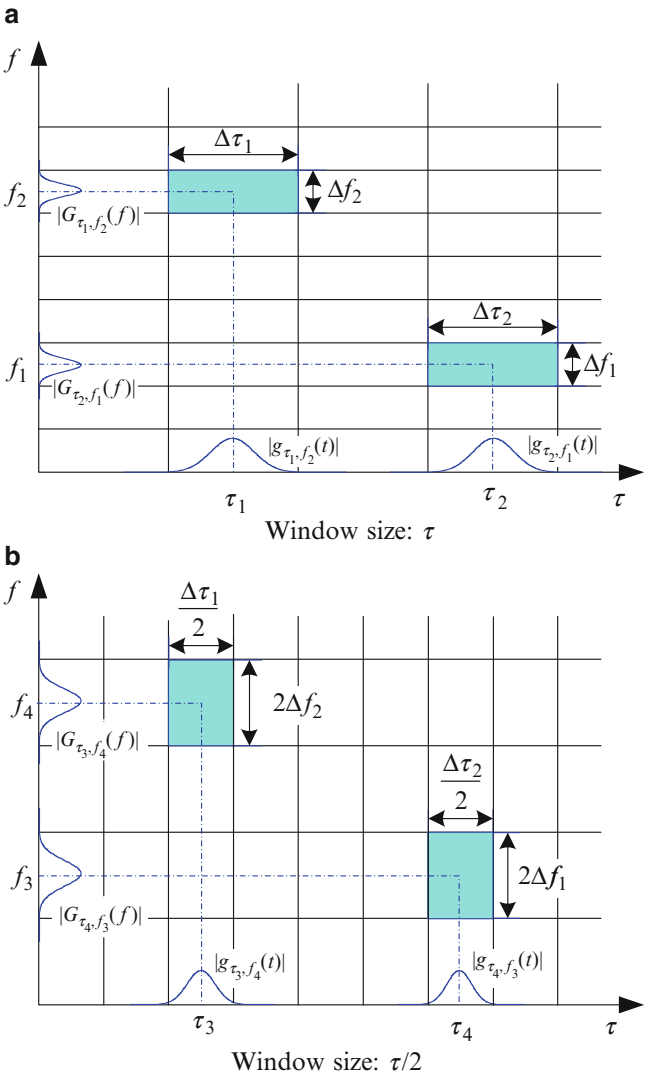

Fig. 2.7 Time-frequency resolutions associated with the STFT technique. (**a**) Window size τ and (**b**) window size $\tau/2$

of 25.6 ms provided good frequency resolution to illustrate the two frequency components in Fig. 2.8b. However, the time-resolution was insufficient to differentiate the four pulse trains that are timely separated with a 12-ms interval. The best overall performance is given by the window width of 6.4 ms, shown in Fig. 2.8c, which allowed for all of the transients to be adequately differentiated on the time-frequency plane. Given that the specific frequency content of an

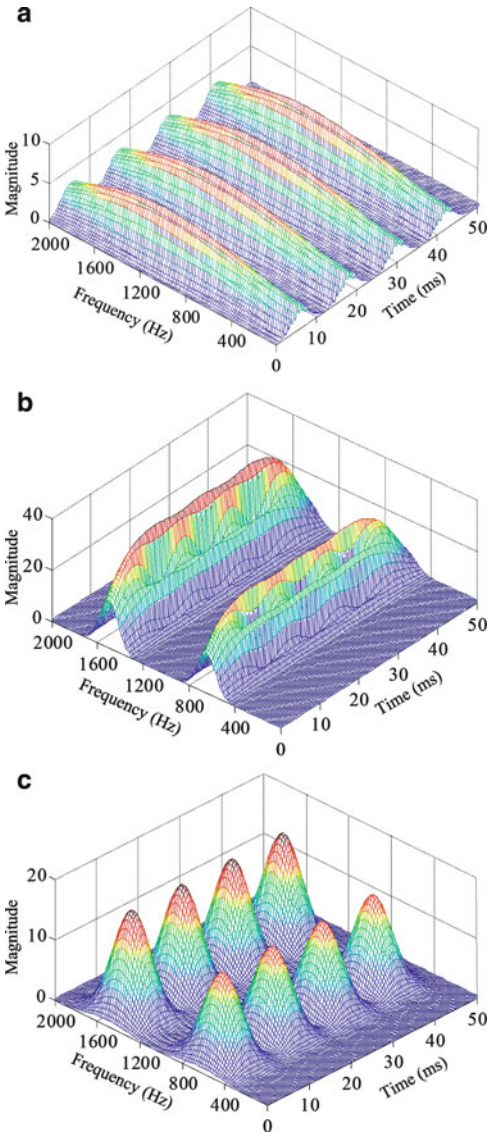

Fig. 2.8 Results of the STFT of the signal using three different window sizes. (**a**) Window size 1.6 ms, (**b**) window size 25.6 ms, and (**c**) window size 6.4 ms

experimentally measured signal is generally not known a priori, selection of a suitable window size for effective signal decomposition using the STFT technique is not guaranteed. The inherent drawback of the STFT motivates researchers to look for other techniques that are better suited for processing nonstationary signals. One of such techniques, which is the focus of this book, is the wavelet transform.

Fig. 2.9 Alfred Haar (1885–1933)

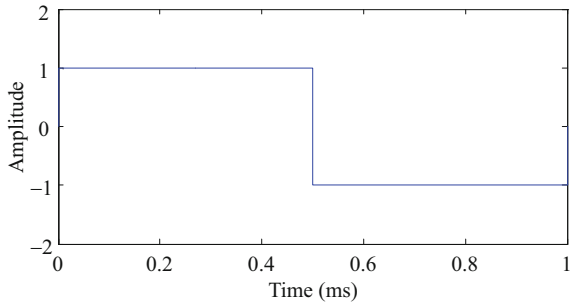

Fig. 2.10 The rectangular basis function

2.3 Wavelet Transform

From a historical point of view, the first reference to the wavelet goes back to the early twentieth century when Alfred Haar (Fig. 2.9) wrote his dissertation titled "On the theory of the orthogonal function systems" in 1909 to obtain his doctoral degree at the University of Göttingen. His research on orthogonal systems of functions led to the development of a set of rectangular basis functions (Haar 1910), as illustrated in Fig. 2.10. Later, an entire wavelet family, the Haar wavelet, was named on the basis of this set of functions, and it is also the simplest wavelet family developed till this date.

Essentially, Haar's basis function consists of a short positive pulse followed by a short negative pulse, and it was used to illustrate a countable orthonormal system for the space of square-integrable functions on the real line (Haar 1910). Later, the Haar basis function was applied to compress images (DeVore et al. 1992).

Little advancement in the field of wavelets was reported after Haar's work, until a physicist, Paul Levy (Fig. 2.11), investigated the Brownian motion in the 1930s. He discovered that the scale-varying function, that is, the Haar basis function, was better suited than the Fourier basis functions for studying subtle details in the Brownian motion. In addition, the Haar basis function can be scaled into different intervals, such as the interval [0, 1] or the intervals [0, 1/2] and [1/2, 1], thereby providing higher precision when modeling a function than that provided by the Fourier basis function, as it can only have one interval $[-\infty, -\infty]$.

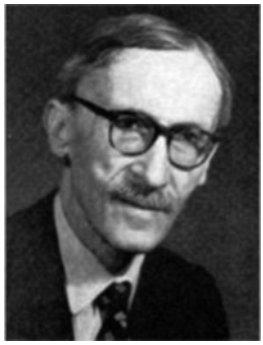

Fig. 2.11 Paul Levy (1886–1971)

Fig. 2.12 Jean Morlet (1931–2007)

While several individuals, such as John Littlewood, Richard Paley (Littlewood and Paley 1931), Elias M. Stein (Jaffard et al. 2001), and Norman H. Ricker (Ricker 1953) have contributed, from the 1930s to the 1970s, to advancing the state of research in wavelets as it is called today, major advancement in the field was attributed to Jean Morlet (Fig. 2.12) who developed and implemented the technique of scaling and shifting of the analysis window functions in analyzing acoustic echoes while working for an oil company in the mid 1970s (Mackenzie 2001). By sending acoustic impulses into the ground and analyzing the received echoes, the existence of oil beneath the earth crust as well as the thickness of the oil layer can be identified. When Morlet first used the STFT to analyze these echoes, he found that keeping the width of the window function fixed did not work. As a solution to the problem, he experimented with keeping the frequency of the window function constant while changing the width of the window by stretching or squeezing the window function (Mackenzie 2001). The resulting waveforms of varying widths were called by Morlet the "Wavelet", and this marked the beginning of the era of wavelet research. As a matter of fact, the approach that Morlet used was similar to what Haar did before, but the theoretical formation of the wavelet transform was first proposed only after Jean Morlet teamed up with Alex Grossmann to work out the idea that a signal could be transformed into the form of a wavelet and then transformed back into its original form without any information loss (Grossmann and Morlet 1984).

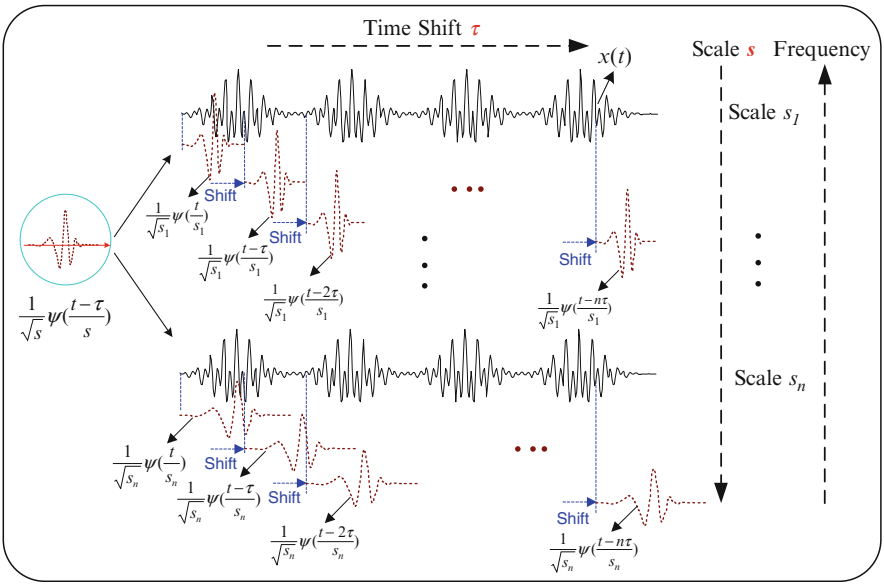

Fig. 2.13 Illustration of wavelet transform

In contrast to the STFT technique where the window size is *fixed*, the wavelet transform enables *variable* window sizes in analyzing different frequency components within a signal (Mallat 1998). This is realized by comparing the signal with a set of template functions obtained from the *scaling* (i.e., dilation and contraction) and *shift* (i.e., translation along the time axis) of a *base* wavelet $\psi(t)$ and looking for their similarities, as illustrated in Fig. 2.13.

Using again the notation of inner product, the wavelet transform of a signal $x(t)$ can be expressed as

$$wt(s,\tau) = \langle x, \psi_{s,\tau} \rangle = \frac{1}{\sqrt{s}} \int_{-\infty}^{\infty} x(t) \psi^* \left(\frac{t-\tau}{s} \right) dt \tag{2.12}$$

where the symbol $s > 0$ represents the scaling parameter, which determines the time and frequency resolutions of the scaled base wavelet $\psi(t-\tau/s)$. The specific values of s are inversely proportional to the frequency. The symbol τ is the shifting parameter, which translates the scaled wavelet along the time axis. The symbol $\psi^*(\cdot)$ denotes the complex conjugation of the base wavelet $\psi(t)$. As an example, if the Morlet wavelet $\psi(t) = e^{i2\pi f_0 t} e^{-(\alpha t^2/\beta^2)}$ is chosen as the base wavelet, its scaled version will be expressed as

$$\psi \left(\frac{t-\tau}{s} \right) = e^{i2\pi f_0 \frac{t-\tau}{s}} e^{-\alpha \frac{(t-\tau)^2}{s^2 \beta^2}} \tag{2.13}$$

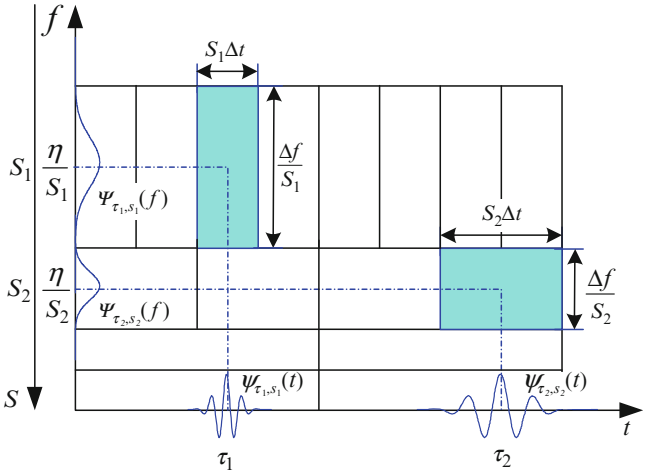

Fig. 2.14 Time and frequency resolutions of the wavelet transform ($s_2 = 2s_1$)

with the parameters f_0, α, and β all being constants. The corresponding time and frequency resolutions of the Morlet wavelet will be calculated as $\Delta t = s\beta/2\sqrt{\alpha}$ and $\Delta f = \sqrt{\alpha}/(s \cdot 2\pi\beta)$, respectively. These expressions indicate that the time and frequency resolutions are directly and inversely proportional to the scaling parameter s, respectively. In Fig. 2.14, variations of the time and frequency resolutions of the Morlet wavelet at two locations on the time–frequency (t–f) plane, $(\tau_1, \eta/s_1)$ and $(\tau_2, \eta/s_2)$, are illustrated.

It is seen that changing the scale from s at the location $(\tau_1, \eta/s_1)$ to $s_2 = 2s_1$ at $(\tau_2, \eta/s_2)$ decreases the time resolution by half (as the width of the time window is doubled) while doubling the frequency resolution (because the width of the frequency window is reduced to half). Through variations of the scale s and time shifts (by τ) of the base wavelet function, the wavelet transform is capable of extracting the constituent components within a time series over its entire spectrum, by using small scales (corresponding to higher frequencies) for decomposing high frequency components and large scales (corresponding to lower frequencies) for low frequency components analysis. As an example, Fig. 2.15 illustrates the result of the wavelet transform performed on the signal shown in Fig. 2.1, using the Morlet base wavelet. It is evident that all the transient components are differentiated in the time scale domain.

Following up the impactful work of Morlet and Grossmann, numerous researchers have invested significant effort in further developing the theory of wavelet transform. Examples include Strömberg's early work on discrete wavelets in 1983 (Strömberg 1983), Grossmann, Morlet, and Paul's work on analyzing arbitrary signals in terms of scales and translations of a single base wavelet function (Grossmann et al. 1985, 1986), and Newman's work on Harmonic wavelet transform in 1993 (Newland 1993). Perhaps the most important step that has led to the prosperity of the wavelets was the invention of multiresolution analysis by

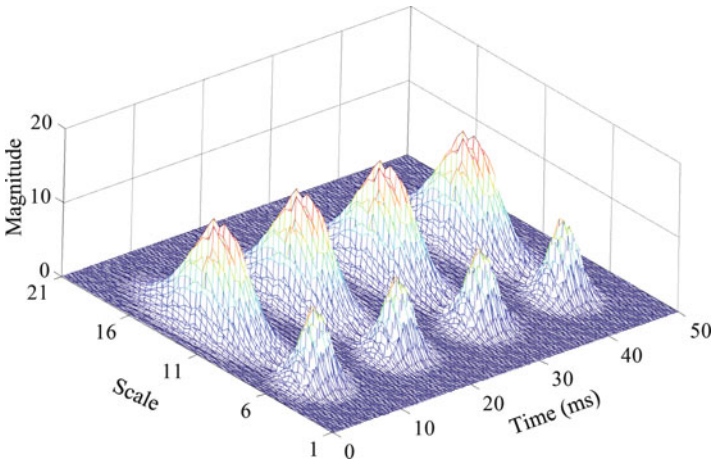

Fig. 2.15 Wavelet transform of the signal

Fig. 2.16 Stephane Mallat

Stephane Mallat (Fig. 2.16) (Mallat 1989a, b, 1999) and Yves Meyer (Fig. 2.17) (Meyer 1989, 1993). Such an invention was introduced by a paper written by Meyer on orthogonal wavelets, entitled "Orthonormal wavelets" (Meyer 1989).

The key to multiresolution analysis is to design the scaling function of the wavelet such that it allowed other researchers to construct their own base wavelets in a mathematically grounded fashion. As an example, Ingrid Daubechies (Fig. 2.18) created her own family of wavelet, the Daubechies wavelets, around 1988 (Daubechies 1988, 1992), on the basis of the concept of multiresolution. Figure 2.19 illustrates one member of the Daubechies wavelet family: Daubechies 2 base wavelet. This type of wavelet is orthogonal and can be implemented using simple digital filtering techniques.

Since then, a proliferation of activities on wavelet transform and its applications in many fields has been seen. These include image processing, speech processing, as well as signal analysis in manufacturing which is the focus of this book.

Fig. 2.17 Yves Meyer

Fig. 2.18 Ingrid Daubechies

Fig. 2.19 Daubechies 2 base wavelet

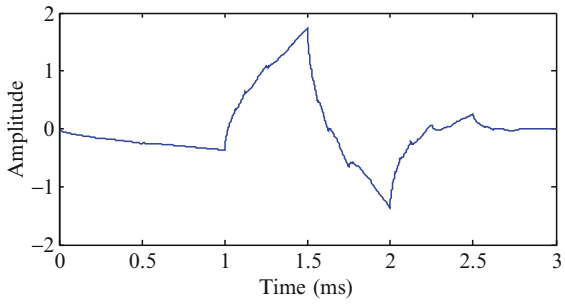

2.4 References

Bracewell, R (1999) The Fourier transform and its applications. 3rd edn. McGraw-Hill, New York
Chui CK (1992) An introduction to wavelets. Academic, New York
Cohen L (1989) Time-frequency distributions – a review. Proc IEEE 77(7):941–981

Cooley JW, Tukey JW (1965) An algorithm for the machine calculation of complex Fourier series. Math Comput 19:297–301
Daubechies I (1988) Orthonormal bases of compactly supported wavelets. Comm Pure Appl Math 4:909–996
Daubechies I (1992) Ten lectures on wavelets. SIAM, Philadelphia, PA
DeVore RA, Jawerth B, Lucier BJ (1992) Image compression through wavelet transform coding. IEEE Trans Inf Theory 38(2):719–746
Fourier J (1822) The analytical theory of heat. (trans: Freeman A). Cambridge University Press, London, p 1878
Gabor D (1946) Theory of communication. J IEEE 93(3):429–457
Grossmann A, Morlet J (1984) Decomposition of hardy functions into square integrable wavelets of constant shape. SIAM J Math Anal 15(4):723–736
Grossmann A, Morlet J, Paul T (1985) Transforms associated to square integrable group representations. I. General results. J Math Phys 26:2473–2479
Grossmann A, Morlet J, Paul T (1986) Transforms associated to square integrable group representations. II: examples. Ann Inst Henri Poincaré 45(3):293–309
Haar A (1910) Zur theorie der orthogonalen funktionen systeme. Math Ann 69:331–371
Herivel J (1975) Joseph Fourier. The man and the physicist. Clarendon Press, Oxford
Jaffard S, Yves Meyer Y, Ryan RD (2001) Wavelets: tools for science & technology. Society for Industrial Mathematics, Philadelphia, PA
Körner TW (1988) Fourier analysis. Cambridge University Press, London
Littlewood JE, Paley REAC (1931) Theorems on Fourier series and power series. J Lond Math Soc 6:230–233
Mackenzie D (2001) Wavelets: seeing the forest and the trees. National Academy of Sciences, Washington, DC
Mallat SG (1989a) A theory of multiresolution signal decomposition: the wavelet representation. IEEE Trans Pattern Anal Mach Intell 11(7):674–693
Mallat SG (1989b) Multiresolution approximations and wavelet orthonormal bases of $L^2(R)$. Trans Am Math Soc 315:69–87
Mallat SG (1998) A wavelet tour of signal processing. Academic, San Diego, CA
Meyer Y (1989) Orthonormal wavelets. In: Combers JM, Grossmann A, Tachamitchian P (eds) Wavelets, time-frequency methods and phase space, Springer-Verlag, Berlin
Meyer Y (1993) Wavelets, algorithms and applications. SIAM, Philadelphia, PA
Newland DE (1993) Harmonic wavelet analysis. Proc R Soc Lond A Math Phys Sci 443(1917) 203–225
Oppenheim AV, Schafer RW, Buck JR (1999) Discrete time signal processing. Prentice Hall PTR, Englewood Cliffs, NJ
Qian S (2002) Time-frequency and wavelet transforms. Prentice Hall PTR, Upper Saddle River, NJ
Ricker N (1953) The form and laws of propagation of seismic wavelets. Geophysics 18:10–40
Rioul O, Vetterli M (1991) Wavelets and signal processing. IEEE Signal Process Mag 8(4):14–38
Strömberg JO (1983) A modified Franklin system and higher-order spline systems on R^n as unconditional bases for Hardy space. Proceedings of Conference on Harmonic Analysis in Honor of Antoni Zygmund, vol 2, pp 475–494
Jean B. Joseph Fourier, http://mathdl.maa.org/images/upload_library/1/Portraits/Fourier.bmp
Dennis Gabor, http://nobelprize.org/nobel_prizes/physics/laureates/1971/gabor-autobio.html
Alfred Haar, http://www2.isye.gatech.edu/∼brani/images/haar.html
Paul Levy, http://www.todayinsci.com/L/Levy_Paul/LevyPaulThm.jpg
Jean Morlet, http://www.industrie-technologies.com/GlobalVisuels/Local/SL_Produit/Morlet.jpg
Stephane Mallat, http://www.cmap.polytechnique.fr/∼mallat/Stephane.jpg
Yves Meyer, http://www.academie-sciences.fr/membres/M/Meyer_Yves.htm
Ingrid Daubechies, http://commons.princeton.edu/ciee/images/people/DaubechiesIngrid.jpg

http://www.springer.com/978-1-4419-1544-3

Wavelets
Theory and Applications for Manufacturing
Gao, R.X.; Yan, R.
2011, XIV, 224 p., Hardcover
ISBN: 978-1-4419-1544-3